

## $\phi_s$ status and prospects at LHCb

---

**Ekaterina Govorkova**\*†

*Nikhef National Institute for Subatomic Physics, Amsterdam, Netherlands*

*E-mail:* [egovorko@nikhef.nl](mailto:egovorko@nikhef.nl)

Recent measurements of the time-dependent CP violation by the LHCb experiment are presented. The decays of  $B_s$  mesons to  $J/\psi K^+ K^-$  and  $J/\psi \pi^+ \pi^-$  final states are used to measure the CP-violating phase  $\phi_s$  in tree-dominated transitions, while  $B_s^0 \rightarrow (K^+ \pi^-)(K^- \pi^+)$  and  $B_s^0 \rightarrow \phi \phi$  decay modes are used to measure the CP-violating phases  $\phi_s^{sd\bar{d}}$  and  $\phi_s^{ss\bar{s}}$ , which arise in penguin-dominated decays. The most recent status of the analyses of the four decay modes is summarised.

*18th International Conference on B-Physics at Frontier Machines - Beauty2019 -  
29 September / 4 October, 2019  
Ljubljana, Slovenia*

---

\*Speaker.

†On behalf of the LHCb Collaboration

## 1. CP violation in the $B_s^0 - \bar{B}_s^0$ system

The CP-violating phase  $\phi_s$  arises in the interference between the  $b \rightarrow c\bar{c}s$  decay amplitudes of  $B_s^0$  meson<sup>1</sup> transitioning directly to its final state or after it has first oscillated to its anti-particle, a  $\bar{B}_s^0$  meson. In the Standard Model (SM), ignoring subleading penguin contributions,  $\phi_s = -2\beta_s$ , where the value of  $\beta_s$  is inferred from global fits to experimental data to be  $-0.0370^{+0.0008}_{-0.0007}$  rad [1, 2]. Such a precise prediction for the  $\phi_s$  value in the SM makes its measurement particularly interesting because new physics processes, if new particles were to contribute to the  $B_s^0 - \bar{B}_s^0$  mixing diagram [3, 4], could potentially modify the phase. Penguin-dominated  $b \rightarrow s\bar{s}s$  and  $b \rightarrow sd\bar{d}$  transitions are described by a phase which is referred to as  $\phi_s^{s\bar{s}s}$  and  $\phi_s^{sd\bar{d}}$ . Unlike  $\phi_s$  from  $b \rightarrow c\bar{c}s$  transition, penguin phases are expected at first order to be exactly zero in the SM. If  $\phi_s$  is measured to be significantly different from the value predicted by the SM, then it would be a clear sign for new physics.

## 2. Measurement of $\phi_s$ at LHCb

The LHCb detector [5, 6] is a general purpose detector in the forward region, situated at the Large Hadron Collider at CERN. The broad physics program of the LHCb experiment covers various topics including study of the CP violation (CPV) in  $B$  mesons. The measurements covered in this manuscript are measurements of the CP-violating phases of the following four decay modes:  $B_s^0 \rightarrow J/\psi K^+ K^-$  [7],  $B_s^0 \rightarrow J/\psi \pi^+ \pi^-$  [8],  $B_s^0 \rightarrow (K^+ \pi^-)(K^- \pi^+)$  [9] and  $B_s^0 \rightarrow \phi \phi$  [10]. The results obtained with  $B_s^0 \rightarrow J/\psi K^+ K^-$  and  $B_s^0 \rightarrow J/\psi \pi^+ \pi^-$  modes were first presented at the 54<sup>th</sup> Rencontres de Moriond conference [11].

### 2.1 Measurement of $\phi_s$ in $b \rightarrow c\bar{c}s$ transition

Two recent measurements of the CP-violating phase  $\phi_s$  using  $B_s^0$  mesons at the LHCb experiment are presented. One analysis explores the  $B_s^0 \rightarrow J/\psi K^+ K^-$  decay mode [7], while the other studies the  $B_s^0 \rightarrow J/\psi \pi^+ \pi^-$  decay [8]. Since the analysis strategies are very similar, the baseline strategy adopted by both is covered and relevant differences between the two are highlighted.

Both analyses use proton-proton collision data collected with the LHCb detector in 2015 and 2016, corresponding to a total integrated luminosity of  $1.9 \text{ fb}^{-1}$ . A  $B_s^0$  ( $\bar{B}_s^0$ ) meson after being produced in a proton-proton collision in the LHCb detector (so-called primary vertex), flies approximately 1 cm before decaying inside the vertex locator, VELO, of the LHCb detector. The excellent decay time resolution of the VELO detector, which is approximately 45.5 (41.5) fs for the  $B_s^0 \rightarrow J/\psi K^+ K^-$  ( $B_s^0 \rightarrow J/\psi \pi^+ \pi^-$ ) mode, allows to resolve oscillations in the  $B_s^0 - \bar{B}_s^0$  system. The decay products of a  $B_s^0$  ( $\bar{B}_s^0$ ) meson,  $J/\psi K^+ K^-$  or  $J/\psi \pi^+ \pi^-$  where  $J/\psi$  decays to a  $\mu^+ \mu^-$  pair, fly from the decay point of  $B_s^0$  (so-called secondary vertex) through the rest of the detector, traversing the magnet, where tracks of charge particles are bent; tracking stations; Cherenkov detectors, which allows to identify hadron type; calorimeter system and muon stations. The distance between the secondary and primary vertices is translated to the  $B_s^0$  meson decay time using an estimate of its momentum.

<sup>1</sup>The inclusion of charge-conjugate processes is implied throughout this manuscript, unless otherwise noted.

The CP-violating parameters  $\phi_s$  and  $|\lambda|$  are measured, where  $|\lambda|$  is defined as  $|\lambda| = \left| \frac{q}{p} \right| \left| \frac{\bar{A}}{A} \right|$ . The  $B_s^0 \rightarrow J/\psi K^+ K^-$  channel allows measuring the lifetime parameters of the  $B_s^0$  meson: the decay-width difference between the light and heavy  $B_s^0$  meson eigenstates,  $\Delta\Gamma_s = \Gamma_L - \Gamma_H$ , and the average decay-width of the states,  $\Gamma_s = \frac{\Gamma_L + \Gamma_H}{2}$ . However, since the  $J/\psi \pi^+ \pi^-$  final state is almost entirely CP-odd [12], only decays of the heavy  $B_s^0$  meson eigenstate are possible, therefore one can measure  $\Gamma_H$  with  $B_s^0 \rightarrow J/\psi \pi^+ \pi^-$ . In order to disentangle the CP-even from the CP-odd component in  $B_s^0 \rightarrow J/\psi K^+ K^-$ , an angular analysis is required. For a four-body final state, three independent angles are needed to describe the system.

The experimental differential decay-time rate for an initial  $B_s^0$  meson as a function of decay time ( $t$ ) and helicity angles ( $\Omega$ ) is given as [13]

$$\frac{d^4\Gamma}{dt d\Omega} \propto \sum_{k=1}^{10} \varepsilon(t, \Omega) f_k(\Omega) h_k(t) \otimes G(t|\sigma_t), \quad (2.1)$$

where  $\varepsilon(t, \Omega)$  is efficiency as a function of decay-time and angular observables,  $f_k(\Omega)$  are angular functions,  $G(t|\sigma_t)$  is experimental decay-time resolution and the decay-time-dependent functions  $h_k(t)$  for the decay of  $B_s^0$  meson produced as  $B_s^0$  meson are given as

$$h_k(t) = \frac{3}{4\pi} e^{-\Gamma t} \left\{ a_k \cosh \frac{\Delta\Gamma t}{2} + b_k \sinh \frac{\Delta\Gamma t}{2} + c_k \cos(\Delta m t) + d_k \sin(\Delta m t) \right\}. \quad (2.2)$$

For an initial  $\bar{B}_s^0$  at production, the signs of  $c_k$  and  $d_k$  should be reversed. The end goal is to perform a simultaneous maximum likelihood fit to the decay-time and three angles in order to extract the CP-violating parameters. As can be seen from equation 2.1, there are several experimental inputs that are required for the time-dependent fit to be performed: efficiency, decay-time resolution of the detector and the knowledge of the flavour of the  $B_s^0$  meson at production. The details on these inputs are given in the following.

### 2.1.1 Selection and mass fit

The time-dependent angular fit is performed on background-subtracted data. For both decays under study a corresponding boosted decision tree [14], BDT, is used to select signal and reject background candidates. The BDTs are trained using data sidebands as background proxy and simulated events as signal proxy. After the training, the optimal cut is found and applied on the data sample.

The main peaking background is due to the  $\Lambda_b^0 \rightarrow J/\psi p K^-$  decays. It can happen that the proton in the final state is mis-identified as a kaon and resulting  $J/\psi K^+ K^-$  wrong combination might end up peaking under the signal peak. Since this contribution is significant for the  $B_s^0 \rightarrow J/\psi K^+ K^-$  mode it is subtracted by injecting negatively weighted simulated  $\Lambda_b^0 \rightarrow J/\psi p K^-$  decays with a total weight equal to the expected contribution of the  $\Lambda_b^0$  background. Other peaking background contributions coming from decays  $B^0 \rightarrow J/\psi K^+ K^-$ ,  $B^0 \rightarrow J/\psi \pi^+ \pi^-$  and  $B^0 \rightarrow J/\psi K^{*0} (\rightarrow K^+ \pi^-)$  are either vetoed using particle identification requirements or accounted for directly in the mass fit.

In order to subtract the combinatorial background, signal weights are used. These weights are obtained using the *s*Plot procedure [15], which assigns a weight to each event based on the probability density function (PDF) that is used to describe the invariant mass spectra. The invariant

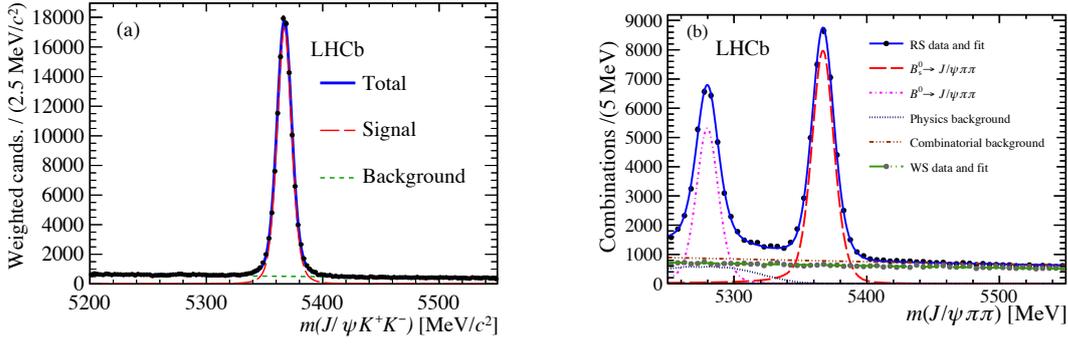


**Figure 1:** Distribution of the invariant mass of selected (a)  $B_s \rightarrow J/\psi K^+ K^-$  [7] and (b)  $B_s \rightarrow J/\psi \pi^+ \pi^-$  [8] decays.

mass distributions of  $J/\psi K^+ K^-$  and  $J/\psi \pi^+ \pi^-$  are shown in Fig. 1 together with the analytical shapes that are used to extract signal weights.

### 2.1.2 Decay time resolution

The decay-time resolution of the detector directly affects the precision of the measured CP-violating parameters. Therefore, detailed understanding of the time resolution is required. The decay-time error that is estimated on an event-by-event basis during the reconstruction step is underestimated and therefore requires calibration. In order to perform the decay-time resolution calibration both analyses use a prompt data sample that consists of  $J/\psi \rightarrow \mu^+ \mu^-$  candidates that originate from the primary vertex and therefore have zero lifetime. The selected  $J/\psi$  candidates are combined with a pair of oppositely charged kaons to mimic the signal decay mode. The decay-time distribution of prompt  $B_s^0 \rightarrow J/\psi K^+ K^-$  candidates is shown in Fig. 2 (a). Events with negative lifetime are present which can only be possible due to the resolution effect of the detector. This is used to assess the effective decay-time resolution of the detector. In order to correct the decay-time uncertainty estimation, a binned procedure is implemented where the prompt sample is divided in several subsamples with different values of the per-event error. In each subsample the effective resolution is assessed by fitting the decay-time distribution. The result of this procedure is shown in Fig. 2 (b). The relation between the effective resolution and the per-event error is parametrised with a linear dependency and the linear calibration parameters are extracted using a  $\chi^2$  fit.

### 2.1.3 Reconstruction and selection efficiency

The geometry of the detector together with the selection requirements cause a non-uniform efficiency as a function of the observables (three helicity angles and decay-time). In the case of the  $B_s^0 \rightarrow J/\psi \pi^+ \pi^-$  decay, the invariant mass of the 2 pions system is also an observable in the fit and the efficiency as a function of it is studied separately. For both decay modes, the efficiency as a function of decay angles is evaluated using simulated samples and then taken into account in the final fit.

The non-uniform shape of the efficiency as a function of decay-time is caused by a biasing selection introduced already in the trigger stage and is described with cubic splines. A data-driven method using the control channel  $B^0 \rightarrow J/\psi K^{*0}$  is adopted to model the decay-time efficiency.

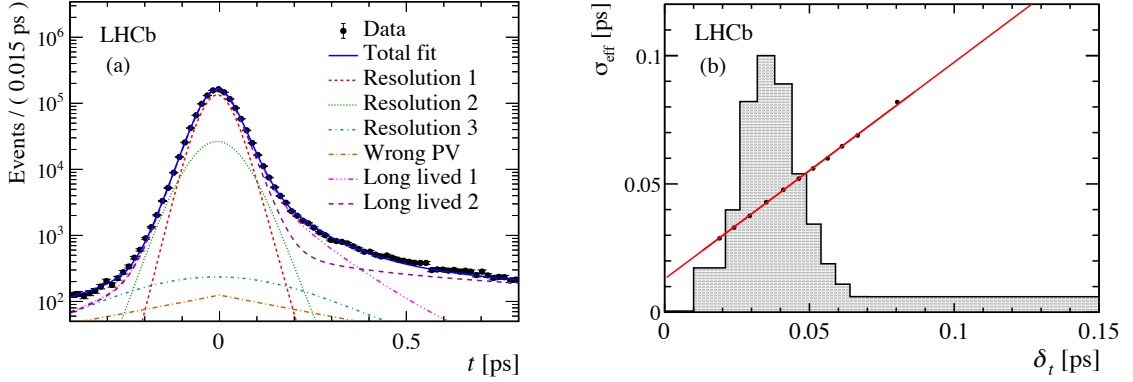


**Figure 2:** (a) Decay-time distribution of the prompt  $B_s \rightarrow J/\psi K^+ K^-$  calibration sample [7] with the result of an unbinned maximum likelihood fit overlaid in blue. The overall resolution is represented by the dashed red line. (b) Variation of the effective decay-time resolution,  $\sigma_{\text{eff}}$ , as a function of the estimated per-candidate decay-time uncertainty,  $\delta_t$ . The red line shows the result when fitting a linear function. The shaded histogram shows the normalized distribution of  $\delta_t$ .

The control channel  $B^0 \rightarrow J/\psi K^{*0}$  is used since it has a well-known lifetime and kinematics of the decay is similar to the signal channels. Using this control channel, decay-width difference between the  $B_s^0$  ( $B_H$ ) and  $B^0$  meson to be determined. This allows the value of the  $\Gamma_{s/H}$  to be extracted using the latest world average of the value of  $\Gamma_{B^0}$ . Signal candidates of the control channel are selected following the selection procedure used for the signal channel. Then the decay-time acceptance is evaluated and corrected by the ratio of acceptances in simulated signal and control channels to take into account differences between the two channels. The final efficiency is represented in the following form:

$$\epsilon_{\text{data}}^{B_s}(t) = \epsilon_{\text{data}}^{B^0}(t) \times \frac{\epsilon_{\text{sim}}^{B_s}(t)}{\epsilon_{\text{sim}}^{B^0}(t)}, \quad (2.3)$$

The differential decay-time rate is then multiplied with evaluated efficiency as shown in equation 2.1.

### 2.1.4 Results

Taking into account all the inputs described above, a time-dependent maximum likelihood fit is performed in order to extract the parameters of interest. Table 1 summarises parameter estimates obtained by the both analyses.

Using a minimum  $\chi^2$  fit, these results are combined with all the previous measurements of the  $\phi_s$  phase performed by the LHCb experiment [16–19]. The combined values are

$$\begin{aligned} \phi_s &= -0.040 \pm 0.025 \text{ [rad]}, \\ |\lambda| &= 0.991 \pm 0.010, \\ \Gamma_s - \Gamma_{B^0} &= -0.0024 \pm 0.0018 \text{ ps}^{-1}, \\ \Delta\Gamma_s &= 0.0813 \pm 0.0048 \text{ ps}^{-1}. \end{aligned} \quad (2.4)$$

**Table 1:** Parameters estimates obtained with  $B_s \rightarrow J/\psi K^+ K^-$  and  $B_s \rightarrow J/\psi \pi^+ \pi^-$  decay modes. The first uncertainty is statistical and the second one is systematic.

	$B_s \rightarrow J/\psi K^+ K^-$	$B_s \rightarrow J/\psi \pi^+ \pi^-$
$\phi_s$ , [rad]	$-0.080 \pm 0.041 \pm 0.006$	$-0.057 \pm 0.060 \pm 0.011$
$ \lambda $	$1.006 \pm 0.016 \pm 0.006$	$1.01^{+0.08}_{-0.06} \pm 0.03$
$\Gamma_{s/H} - \Gamma_{B^0}$ , [ps <sup>-1</sup> ]	$-0.0041 \pm 0.0024 \pm 0.0015$	$-0.050 \pm 0.004 \pm 0.004$
$\Delta\Gamma_s$ , [ps <sup>-1</sup> ]	$0.0772 \pm 0.0077 \pm 0.0026$	-

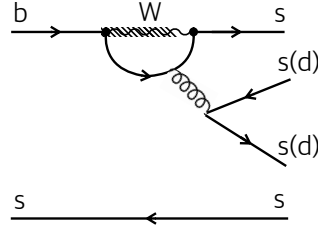


**Figure 3:** Feynman diagram for  $b \rightarrow ss\bar{s}$  ( $b \rightarrow sd\bar{d}$ ) penguin transition.

The results are compatible with the SM expectations and with no CPV in the decay modes under study.

## 2.2 The CP-violating phases $\phi_s^{sd\bar{d}}$ and $\phi_s^{ss\bar{s}}$

Two recent measurements performed by the LHCb Collaboration of the CP-violating phases  $\phi_s^{sd\bar{d}}$  and  $\phi_s^{ss\bar{s}}$ , arising in the penguin dominated decays, are presented. One analysis explores the  $B_s^0 \rightarrow (K^+ \pi^-)(K^- \pi^+)$  decay mode [9], while the other studies the  $B_s^0 \rightarrow \phi\phi$  decay [10]. Both decays can only proceed via penguin transition via either  $b \rightarrow ss\bar{s}$  or  $b \rightarrow sd\bar{d}$ , with corresponding Feynman diagram shown in Fig. 3. The CP-violating phases  $\phi_s^{sd\bar{d}}$  and  $\phi_s^{ss\bar{s}}$  that arise in those transitions are expected in the first order to be zero, according to the SM.

**Table 2:** Parameters estimates obtained with  $B_s^0 \rightarrow (K^+ \pi^-)(K^- \pi^+)$  and  $B_s^0 \rightarrow \phi\phi$  decay modes. The first uncertainty is statistical and the second one is systematic.

	$B_s^0 \rightarrow (K^+ \pi^-)(K^- \pi^+)$	$B_s^0 \rightarrow \phi\phi$
$\phi_s^{penguin}$ , rad	$-0.10 \pm 0.13 \pm 0.14$	$-0.07 \pm 0.13 \pm 0.03$
$ \lambda $	$1.035 \pm 0.034 \pm 0.089$	$1.02 \pm 0.05 \pm 0.03$

Both analyses use proton-proton collision data collected with the LHCb detector in Run 1 period (2011-2012), which corresponds to a total integrated luminosity of 3 fb<sup>-1</sup>. And  $B_s^0 \rightarrow \phi\phi$  analysis exploits in addition the 2015 and 2016 datasets, corresponding to a total integrated luminosity of 1.9 fb<sup>-1</sup>. The invariant mass spectra for the both decay modes are shown in Fig. 4. Table 2 summarises parameter estimates obtained by the both analyses. The obtained results are in agreement with the SM expectations.

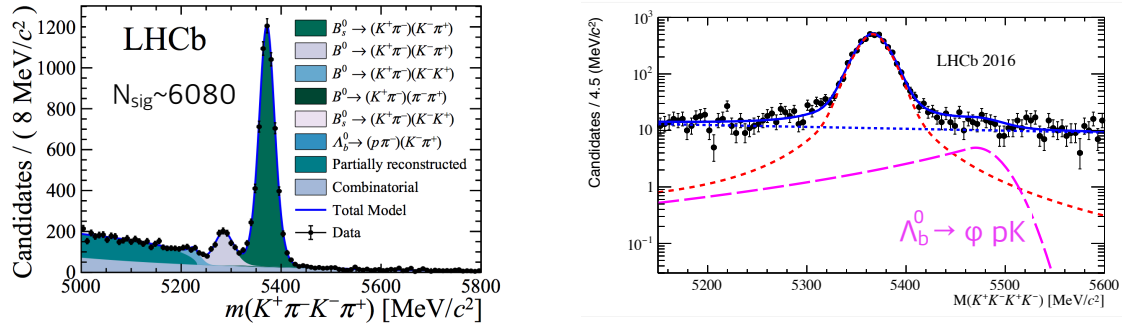


**Figure 4:** Distribution of the invariant mass of selected (a)  $B_s^0 \rightarrow (K^+ \pi^-)(K^- \pi^+)$  [9] and (b)  $B_s^0 \rightarrow \phi \phi$  [10] decays.

## References

- [1] CKMfitter Group, *CP violation and the CKM matrix: Assessing the impact of the asymmetric B factories*, *Eur. Phys. J.* **C41** (2005) 1 [hep-ph/0406184].
- [2] UTFIT collaboration, *Unitarity Triangle Analysis and D meson mixing in the Standard Model and Beyond*, *PoS EPS-HEP2017* (2017) 205.
- [3] A. J. Buras, *Flavour Theory: 2009*, *PoS EPS-HEP2009* (2009) 024 [0910.1032].
- [4] C.-W. Chiang, A. Datta, M. Duraisamy, D. London, M. Nagashima and A. Szykman, *New Physics in  $B_s^0 \rightarrow J/\psi \phi$ : A General Analysis*, *JHEP* **04** (2010) 031 [0910.2929].
- [5] LHCb collaboration, *The LHCb Detector at the LHC*, *JINST* **3** (2008) S08005.
- [6] LHCb collaboration, *LHCb Detector Performance*, *Int. J. Mod. Phys.* **A30** (2015) 1530022 [1412.6352].
- [7] LHCb collaboration, *Updated measurement of time-dependent CP-violating observables in  $B_s^0 \rightarrow J/\psi K^+ K^-$  decays*, *Eur. Phys. J.* **C79** (2019) 706 [1906.08356].
- [8] LHCb collaboration, *Measurement of the CP-violating phase  $\phi_s$  from  $B_s^0 \rightarrow J/\psi \pi^+ \pi^-$  decays in 13 TeV pp collisions*, *Phys. Lett.* **B797** (2019) 134789 [1903.05530].
- [9] LHCb collaboration, *First measurement of the CP-violating phase  $\phi_s^{d\bar{d}}$  in  $B_s^0 \rightarrow (K^+ \pi^-)(K^- \pi^+)$  decays*, *JHEP* **03** (2018) 140 [1712.08683].
- [10] LHCb collaboration, *Measurement of CP violation in the  $B_s^0 \rightarrow \phi \phi$  decay and search for the  $B^0 \rightarrow \phi \phi$  decay*, *JHEP* **12** (2019) 155 [1907.10003].
- [11] E. Govorkova, *Mixing and time-dependent CP violation in beauty at LHCb*, 2019, 1905.08465.
- [12] LHCb collaboration, *Analysis of the resonant components in  $B_s^0 \rightarrow J/\psi \pi^+ \pi^-$* , *Phys. Rev.* **D86** (2012) 052006 [1204.5643].
- [13] X. Liu, W. Wang and Y. Xie, *Penguin pollution in  $B \rightarrow J/\psi V$  decays and impact on the extraction of the  $B_s - \bar{B}_s$  mixing phase*, *Phys. Rev.* **D89** (2014) 094010 [1309.0313].
- [14] L. Breiman, J. Friedman, R. A. Olshen and C. J. Stone, *Classification and regression trees*. Chapman and Hall/CRC, 1984.

- [15] M. Pivk and F. R. Le Diberder, *SPlot: A Statistical tool to unfold data distributions*, *Nucl. Instrum. Meth. A* **555** (2005) 356 [[physics/0402083](#)].
- [16] LHCb collaboration, *Measurement of the CP-violating phase  $\phi_s$  in  $\bar{B}_s^0 \rightarrow J/\psi\pi^+\pi^-$  decays*, *Phys. Lett. B* **736** (2014) 186 [[1405.4140](#)].
- [17] LHCb collaboration, *Measurement of the CP violating phase and decay-width difference in  $B_s^0 \rightarrow \psi(2S)\phi$  decays*, *Phys. Lett. B* **762** (2016) 253 [[1608.04855](#)].
- [18] LHCb collaboration, *Measurement of the CP-violating phase  $\phi_s$  in  $\bar{B}_s^0 \rightarrow D_s^+D_s^-$  decays*, *Phys. Rev. Lett.* **113** (2014) 211801 [[1409.4619](#)].
- [19] LHCb collaboration, *Resonances and CP violation in  $B_s^0$  and  $\bar{B}_s^0 \rightarrow J/\psi K^+K^-$  decays in the mass region above the  $\phi(1020)$* , *JHEP* **08** (2017) 037 [[1704.08217](#)].